

Hurricane Beryl Building Footprint, Structural Damage, and Debris Assessment

Executive Summary

Hurricane Beryl caused widespread damage across the Caribbean, highlighting the urgent need for scalable, rapid, and transparent damage assessment methods to support emergency response and recovery. This report demonstrates how open and commercial Earth observation (EO) data can be integrated to estimate building damage and debris volume in data-sparse, cloud-prone environments. Using building footprint analysis, Sentinel-1 coherent change detection (CCD), and digital surface models (DSM), we developed a low-latency workflow that offers critical situational awareness even when traditional optical imagery is unavailable or incomplete. While each data source has limitations, their combined use reveals meaningful insights and scalable pathways forward. Key findings include:

Building Footprint Mapping

- SAM-derived footprints from VHR imagery provide the most accurate baseline.
- Open datasets like Google and VIDA overestimate structures, while Microsoft's are more conservative but often outdated.

Damage Detection with Sentinel-1

- CCD effectively identifies damage hot spots across large areas, even under heavy vegetation or cloud cover.
- Performance varies by urban density and vegetation, with partial alignment to Copernicus EMS damage labels.

Debris Volume Estimation

- OSM building heights are systematically underestimated; DSM-based heights are affected by post-event damage.
- A combined approach using both sources—along with assumptions on material composition—is recommended.

Recommended Next Steps

- **Use SAM or similar tools** to generate region-specific building footprints.
- **Adopt Sentinel-1 CCD** as a rapid assessment tool to guide further investigation.
- **Develop algorithms** for classifying damage based on DSM height distributions.
- **Acquire VHR SAR or lidar data** where precision is critical.
- **Refine debris estimates** with local data on construction types and field validation.

These findings support UNOPS' efforts to operationalize open EO data for disaster response and promote resilient, data-informed recovery strategies across hurricane-prone regions.

1. Introduction

Hurricane Beryl, one of the earliest and most intense storms of the 2024 Atlantic season, inflicted severe damage across the Caribbean, particularly in Grenada and Saint Vincent and the Grenadines. High winds and torrential rains destroyed homes, schools, and public infrastructure, leaving many communities without shelter, power, or access to essential services. The storm's impacts were especially pronounced in vulnerable areas where informal settlements, subsistence livelihoods, and limited emergency response capacity intersected. In coastal and low-lying regions, localized storm surges compounded structural losses and displaced entire neighborhoods. As national authorities and international partners mobilize resources, it is essential that damage assessments reflect not only the spatial extent of destruction but also the differentiated vulnerabilities that shape community recovery trajectories.

Accurate post-disaster assessments remain constrained by several technical challenges. Optical satellite imagery, while useful for visual interpretation, is frequently cloud-obstructed in tropical cyclone events. Complex damage signatures—such as fragmented building debris, vegetative cover masking destruction, or partial collapse—pose further obstacles for automated detection. Ground surveys, although vital, are resource-intensive and often infeasible across dispersed island geographies. These challenges hinder real-time decision-making and risk underestimating both the severity and spatial distribution of hurricane impacts. The need for scalable, open-source damage mapping tools is especially urgent in the context of rapidly intensifying climate hazards.

To meet this need, UNOPS is providing geospatial and analytical support to emergency response and reconstruction efforts in affected countries, with the Peace and Security Cluster (PSC) leading efforts in Grenada and Saint Vincent and the Grenadines. This report contributes to those efforts by providing: (1) an independent assessment of building footprint presence to establish pre-storm exposure; (2) a damage assessment using open geospatial data—including synthetic aperture radar and optical imagery—to identify affected structures; and (3) an estimation of building debris volume and material mass stock resulting from Beryl's destruction. Together, these assessments demonstrate how open EO data can support sustainable, equitable, and scientifically rigorous disaster response and recovery in the Caribbean and other hazard-prone regions.

2. Building footprint dataset comparison and generation

Accurate building footprint data are essential for estimating storm exposure, mapping structural damage, and quantifying debris in the aftermath of disasters like Hurricane Beryl. However, the reliability of open geospatial building datasets varies widely across regions, particularly in small island and coastal environments where structures are densely packed, informally constructed, or interspersed with vegetation. To establish a baseline of built environment exposure prior to Hurricane Beryl, we conducted a comparative analysis of publicly available building footprint datasets. This comparison enables a critical evaluation of coverage, precision, and consistency

across sources, informing downstream damage and debris estimates and identifying best practices for footprint selection in future disaster response workflows.

We downloaded and evaluated three widely used open geospatial products: Google's Open Buildings dataset (sites.research.google.com/gr/open-buildings), Microsoft's Global Building Footprints (planetarycomputer.microsoft.com/dataset/ms-buildings), and a hybrid dataset combining both sources, VIDA (source.coop/repositories/vida/google-microsoft-open-buildings/description). These datasets differ in spatial coverage, detection methods, and resolution, which can influence downstream estimates of damage and debris. By systematically comparing their footprint density, distribution, and overlap across affected areas in Grenada and Saint Vincent and the Grenadines, we assessed their suitability for post-disaster infrastructure assessments and informed the selection of a reference dataset for our subsequent analysis.

In addition to evaluating existing building footprint datasets, we generated our own building footprint layer using the Segment Anything Model (SAM), an open-source segmentation model developed by Meta AI. Leveraging very-high-resolution (50 cm) satellite imagery acquired on May 6, 2022, and December 10, 2023, we applied a multi-shot segmentation strategy to detect and delineate individual buildings across selected areas in Grenada and Saint Vincent and the Grenadines. This approach allowed us to tailor footprint extraction to local urban morphologies, particularly in regions where open datasets showed gaps or inconsistencies. The use of multi-temporal imagery helped validate the persistence of structures over time, while SAM's flexible prompt-based interface enabled semi-automated, fine-tuned segmentation well-suited for small-island environments with diverse building types and densities.

Comparison across datasets

The count and average size of building footprints varied considerably across datasets, underscoring key trade-offs between spatial coverage and mapping accuracy. Google's Open Buildings dataset identified 9,987 structures in the study area, but many of these detections appear to be false positives—frequently mislabeling ships, vegetation, or small impermanent objects as buildings. This overestimation results in an inflated footprint count and a smaller average footprint size of 82.5 square meters (Figures 1-2). In contrast, Microsoft's Global Building Footprints adopted a more conservative approach, detecting 5,949 structures with a considerably larger average area of 117 square meters—suggesting an emphasis on well-defined, complete buildings and fewer spurious detections (Figure 3). VIDA, a hybrid dataset combining Google and Microsoft products, produced an even higher count of 10,913 structures, though its average footprint size remained nearly identical at 83.1 square meters. The spatial patterns of VIDA closely mirrored those of Google, inheriting its tendency to over-detect and misclassify small features (Figure 4).

SAM applied to 50-cm very-high-resolution imagery generated the smallest number of structures (4,980) but the largest average footprint at 188 square meters (Figure 5). SAM's

segmentation likely captures full building complexes or densely arranged structures, particularly common in urban Caribbean contexts. While lower in count, these SAM-derived footprints may offer a more realistic representation of the built environment, highlighting the value of locally tuned, high-resolution segmentation for post-disaster analysis compared to ready-made building footprint datasets (Figure 6).

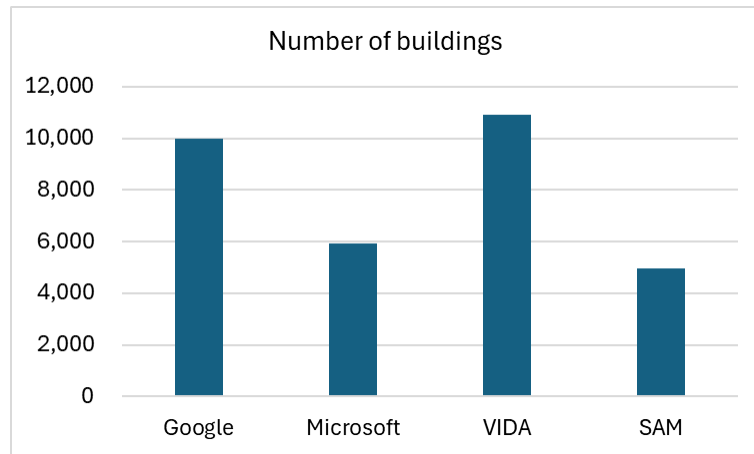


Figure 1. Comparison between Google Open Buildings dataset, Microsoft Global Building Footprints, VIDA, and SAM model identified building footprints



Figure 2. Google Open Buildings building footprints.



Figure 3. Microsoft Global Building Footprints.



Figure 4. VIDA building footprints.

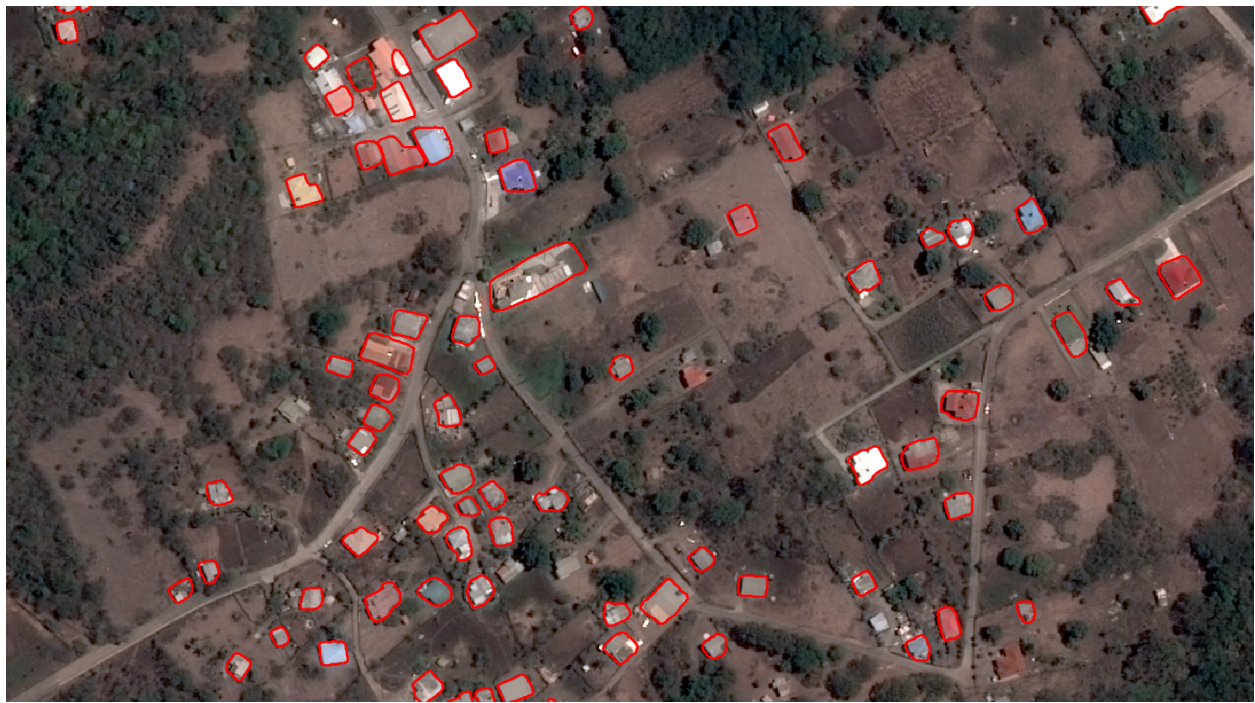


Figure 5. SAM building footprints.





Figure 6. Example overlays across all building footprint datasets.

Summary and Recommendations

Our comparative analysis of four building footprint datasets—Google Open Buildings, Microsoft Global Building Footprints, VIDA, and custom outputs from the SAM model—reveals notable differences in structure count, footprint size, and spatial accuracy. Each dataset offers distinct advantages and limitations, with important implications for post-disaster exposure mapping and debris estimation.

Google's Open Buildings dataset provides wide spatial coverage but consistently overestimates the number of structures, often misclassifying small, non-building objects such as vehicles, vegetation clusters, or marine vessels as buildings. This leads to an inflated footprint count and underestimation of average building size, which can distort downstream damage assessments.

Microsoft's Global Building Footprints dataset is more conservative in structure count and generally avoids the small-object commission errors seen in Google and VIDA. However, a substantial number of Microsoft footprints are misaligned with current very-high-resolution (VHR) imagery, likely due to outdated source data. This misalignment limits its usefulness for precise damage assessment or exposure estimation unless corrected with recent imagery.

VIDA, a hybrid product that merges Google and Microsoft datasets, inherits Google's biases almost entirely. While it offers a slightly higher structure count, its average footprint size and spatial distribution are virtually indistinguishable from Google's. As such, VIDA offers no clear advantage and should be treated with similar caution.

SAM-generated footprints, created using 50-cm VHR imagery, produced the most realistic representation of the built environment, with larger average footprint sizes and clearer delineation of building complexes. However, SAM occasionally over-generalizes, merging adjacent landscape elements—such as parking lots or vegetation patches—into oversized building polygons. Despite these occasional artifacts, SAM outputs were overall the most reliable in reflecting true building presence and layout.

Recommendations: When feasible, we recommend generating a region-specific building footprint layer using SAM or a similar semantic segmentation architecture applied to VHR imagery. This approach offers the highest potential for accurate exposure estimation and integration with damage and debris assessments. Where time, data access, or technical resources limit the use of SAM, Microsoft or Google datasets may be used as alternatives—provided that a minimum area filter (e.g., $>30\text{ m}^2$) is applied to remove small-object false positives and mitigate overcounting. In this context, Microsoft may be preferable if known geolocation issues are corrected. VIDA is not recommended for operational use, as it does not offer improved accuracy or spatial fidelity beyond what is already available in the individual Google and Microsoft datasets.

Data shared in repo

- *Building_footprints_SAM.shp*: SAM-derived building footprints

3. Building damage analysis

Despite the widespread destruction caused by Hurricane Beryl, comprehensive and timely damage assessments across the full extent of affected areas remain limited. Existing products, such as those from the Copernicus Emergency Management Service (EMS), rely on manual photo-interpretation of very high-resolution optical imagery and are constrained by cloud cover and scene availability—leaving large swaths of the impacted region unassessed. To address this gap, we apply a low-latency, scalable damage detection approach using Sentinel-1 synthetic aperture radar (SAR) and coherent change detection (CCD). This method allows us to estimate hurricane-related structural damage even in areas where optical imagery is unavailable or incomplete, providing a more continuous and cost-effective overview of affected zones. By comparing CCD results to available Copernicus EMS data and integrating multiple building footprint datasets, we evaluate the effectiveness of SAR-based monitoring in this unique tropical setting and propose a framework for operationalizing radar-guided post-disaster assessments at regional scales.

Evaluation of existing Copernicus EMS damage data

The Copernicus Emergency Management Service (EMS) produces damage assessments using photo-interpretation of very high resolution (VHR) satellite optical imagery. For Hurricane Beryl and within our region of interest, Copernicus EMS analysts photo-interpreted Pleiades and WorldView-2 data, identifying 1,642 “damaged” buildings, 2,305 “destroyed” buildings, and 1,536 buildings with “possible damage” (<https://rapidmapping.emergency.copernicus.eu/EMSR734>). Copernicus produced these graded damage assessments on some, but not all islands in the affected areas around our study region (Table 1). Copernicus EMS did not produce damage assessments in locations where VHR optical imagery were cloud occluded at the time of initial activation, and the EMS has not revisited the case since. The affected areas delineated by Copernicus EMS where they did **not** produce graded damage data constitute 85.1% of this affected area, meaning that EMS was not able to produce graded damage data for the vast majority of areas it had delineated as affected by Hurricane Beryl.

Table 1. Summary of Copernicus EMS damage assessments.

Activation Area Name	Affected Area (sq km)	Image Date	Graded Damage	Publication Date
Grenada	290.7	4 July 2024	N	N/A
Saint Vincent	155.91	8 July 2024	N	N/A
Bridgetown	73.48	2 July 2024	N	N/A
Carricaou	46.49	2 July 2024	Y	3 July 2024
Union Island	17.11	2 July 2024	Y	5 July 2024

Canouan	12.63	2 July 2024	Y	5 July 2024
Mustique	9.54	4 July 2024	Y	5 July 2024
Petite Martinique	2.83	2 July 2024	Y	3 July 2024
Mayreau	2.56	2 July 2024	Y	5 July 2024

Generation of S1 damage analysis

We used Sentinel-1 data acquired over the region on 7 July 2024 to produce continuous estimates of Sentinel-1-indicated damage using the long temporal arc coherent change detection (CCD) approach we have developed in other settings (Scher & Van Den Hoek, 2025). Low-latency, broad coverage at medium spatial resolution with Sentinel-1 CCD is a key advantage of this method for rapid damage assessment because we can quickly extend damage mapping across the entire affected area where Sentinel-1 data have been acquired.

We combined Sentinel-1 images from different orbital directions: one from ascending track 164 and another from descending track 156. Combining Sentinel-1 acquisitions from different orbital tracks and orientation of illumination can build a more complete record of damage where steep terrain may occlude Sentinel-1 data on from one orbital vantage point but not another. Each of these two Sentinel-1 images acquired after the hurricane were paired with 10 pre-hurricane Sentinel-1 images to estimate interferometric coherence across all ten pre-hurricane images. These coherence estimates were compared to a similar construction of InSAR images pairs for coherence estimation using reference scenes acquired on each orbital path 12-days prior (25 June 2024).

We use pre-hurricane coherence data to delineate areas valid for CCD monitoring. Within our study region, we can monitor with CCD 1,223 (74.5%) of “damage”, 1,678 (72.8%) of “destroyed”, and 1,117 (72.7%) of “possible damage” points produced by Copernicus EMS. This is lower than, for example, our work in the Gaza Strip due to the highly variable pre-hurricane radar scattering characteristics in these tropical Caribbean islands, where Sentinel-1 radar is highly sensitive to the presence of vegetation. The effects of vegetation reduce the areas that CCD can be used to reliably monitor for indicated damage. Our CCD approach delineates broad areas with indicated damage within the study region gridded at the 40m pixel spacing (Figure 7).



Figure 7. Example of CCD-indicated damage raster data at 40m pixel spacing over Saint Vincent and the Grenadines.

Agreement with Copernicus EMS data

Our CCD-based damage detection approach captures just over half (54.0%) of Copernicus EMS points under monitoring within the study region. By graded damage label, we capture 56.3% of “damaged”, 53.5% of “destroyed”, and 36.6% of “possible damage” points with our automated approach. This is on the lowest end of agreement we have achieved in other settings, and we believe this is due to the dense tropical vegetation surrounding relatively small structures in the region. In more densely built-up areas of the study region, CCD does well to detect building-level damage (Figure 8). In less densely built-up areas, CCD tends to miss damage due to the dominant effect of vegetation and moisture dynamics on the pre-hurricane radar scattering signal (Figure 9). We also detect varying aggregate levels of building damage for various building footprint source datasets (Table 2), which are broadly proportionate to the respective building footprint counts of each dataset (Figure 1).



Figure 8. Microsoft building footprints classified as damage by CCD (blue) on Main Street and the surrounding area in Carriacou.



Figure 9. Microsoft building footprints classified as damage by CCD (blue) in central Carriacou. Note visible damage in the basemap image that is missed with CCD-based damage detection in these less densely built-up areas.

Table 2. Summary of CCD-detected damaged buildings by building footprint dataset.

Building Footprint Dataset	Number of Buildings Damaged
Google Open Buildings	3259
Microsoft Global Building Footprints	1960
VIDA building footprints	3474
SAM-generated building footprints	1379

Summary and Recommendations

Our analysis demonstrates both the potential and limitations of using Sentinel-1 coherent change detection (CCD) for post-disaster damage mapping in the aftermath of Hurricane Beryl. Compared to other settings—such as the Gaza Strip, where radar coherence change aligns

closely with photo-interpreted building damage—CCD performance in the Caribbean context is somewhat diminished due to dense tropical vegetation, variable land cover, and small, often informal structures that reduce signal reliability. Despite these constraints, our method successfully captured a substantial portion of Copernicus EMS-identified damage and revealed clear damage hot spots across several affected areas. The key advantage of Sentinel-1 CCD lies in its ability to produce rapid, low-cost, and cloud-agnostic assessments across large spatial extents—making it well suited for identifying broad zones of damage when optical imagery is unavailable or delayed.

Recommendations: To maximize utility, we recommend deploying Sentinel-1 CCD for full regional coverage of hurricane-affected areas, filling significant monitoring gaps left by Copernicus EMS. These assessments can serve either as standalone conservative estimates or as a first step in a “tip-and-cue” framework, in which radar-identified hot spots guide tasking of very-high-resolution (VHR) commercial SAR imagery for detailed, building-level analysis. This layered approach balances speed and precision, enabling operational agencies to move from broad triage to targeted validation and response. When VHR SAR tasking is cost-prohibitive, Sentinel-1 CCD alone still provides valuable, timely insights for emergency managers by reliably detecting zones of concentrated damage under any atmospheric or illumination conditions. We recommend institutionalizing this workflow for future rapid response, especially in cloud-prone or logistically challenging environments.

Data shared in repo

- *Damage/output/beryl_s1_damage_40m.tif*: Gridded 40m Sentinel-1 CCD indicated damage
- *Damage/output/bsar_damage_beryl_{}.geojson*: Building footprints identified with damage using the CCD raster above. There are four GeoJSON files, each corresponding to each of the four building footprint datasets (Microsoft – MSFT, Google – GOOG, VIDA, and SAM)

4. Debris volume and tonnage estimation

Accurately estimating the volume of debris generated by disasters like Hurricane Beryl is essential for effective recovery planning, resource allocation, and environmental impact mitigation. Yet despite its importance, volumetric debris analysis remains one of the most challenging aspects of post-disaster assessment, particularly when relying solely on remote sensing data. While satellite imagery can identify damaged structures and classify debris fields, it typically lacks the vertical resolution needed to measure height, density, or material composition—key inputs for estimating volume and mass. These limitations are especially acute in small island and coastal settings, where buildings vary widely in construction type and topography complicates inference. As a result, volumetric estimates often require combining remote assessments with model-based assumptions or on-the-ground data that are difficult to obtain at scale. This section outlines our approach to bridging these gaps by integrating multiple georeferenced datasets (Figure 10):

- SAM-derived building footprints, described in Section 1 above
- CCD-derived footprint-level damage detection, described in Section 2 above
- Copernicus EMS structural damage data
- Pre-Beryl dataset on building heights from OpenStreetMap (OSM) (available through OneGeo onegeo.co/data for analysis and ESRI <https://www.arcgis.com/home/item.html?id=ca0470dbbddb4db28bad74ed39949e25> for visual inspection)
- Post-Beryl very-high resolution (1 meter) Pleiades satellite image-derived digital surface model (DSM)

We incorporate these data to estimate the volume of structural damage per building footprint and apply standardized assumptions about construction composition and materials to generate first-order estimates of debris volume and tonnage.



Figure 10. Copernicus-labeled damaged structures (upper-left; green); OSM building footprints with attributed pre-event building heights (upper-right; purple); SAM-derived building footprints (lower-left; red); Pleiades stereophotogrammetry-derived 1 meter resolution DSM (lower-right; elevation range: 14-31 masl). Google Earth-hosted background imagery depicts a post-Beryl very-high resolution satellite image. Longitude: -61.488°, latitude: 12.452°.

Estimation of building heights

We first looked at available data to generate pre-Beryl building heights to inform our estimation of debris volume and tonnage. The OSM dataset provided heights at 8198 building footprints, which broadly overlap with SAM-derived building footprints. 7613 (93%) of OSM building footprints have a reported height of 2.8 meters, which is the minimum height across the entire dataset. While the maximum height across OSM building footprints is recorded as 24 meters, there are only 300 building footprints with a height above 5.6 meters. This suggests that the OSM dataset is exceptionally biased and inaccurately attributes a minimally detectable height of

2.8 meters (perhaps representative of a single floor-structure) to all but approximately 500 buildings across the study area.

As an alternative approach, we used the very-high resolution DSM to estimate building height through a simple differencing of the minimum and maximum elevations recorded within each SAM-derived building footprint. The median DSM-derived height of SAM building footprints is 5.2 meters with a mode height of 4.6 meters. Since the DSM was derived using post-Beryl imagery, a likely shortcoming of this approach is that the pre-Beryl maximum elevation of a given structure, as well as the derived height, will be underestimated due to damage inflicted by the storm. This is reflected in the minimum DSM height across SAM building footprints of 0.1 meters. That said, only 703 (9%) SAM building footprints have a height equal to or less than the mode OSM height of 2.8 meters, reflecting the much larger distribution of building heights based on DSM data.

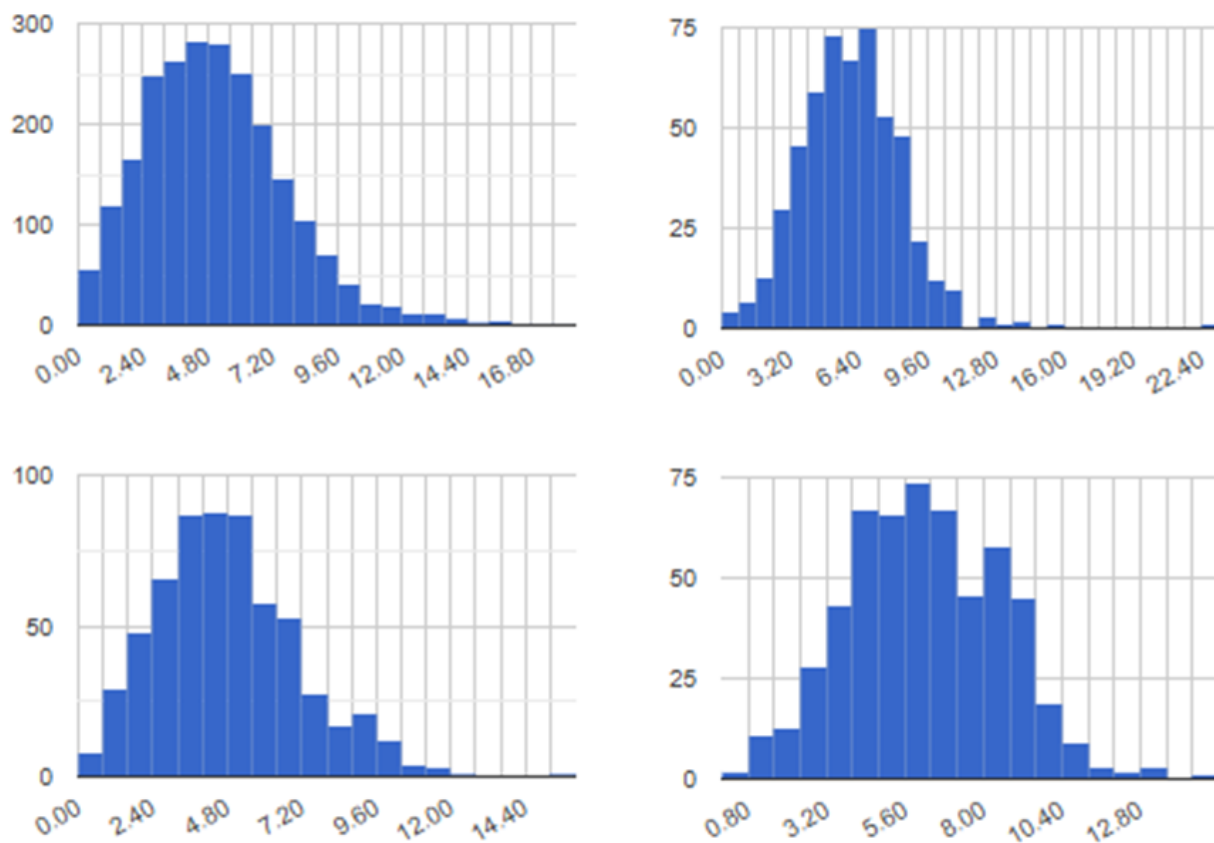


Figure 11. Histograms of building heights for undamaged (upper-left), possibly damaged (upper-right), damaged (lower-left), and destroyed buildings (lower-right). Height data based on the range of DSM elevation values within SAM building footprints. Damage categorization based on Copernicus EMS data.

We compared the OSM and DSM-derived heights by considering undamaged and destroyed, damaged, or possibly damaged structures separately, using the Copernicus EMS damage

dataset as a reference, and measuring DSM heights using OSM building footprints rather than SAM building footprints. We found an exceptionally poor agreement between OSM and DSM-derived building heights for 5331 undamaged OSM buildings (Figure 12a) and 2867 destroyed, damaged, or possibly damaged OSM buildings (Figure 12b). OSM heights saturate prematurely at 2.8 meters in both comparisons but also cluster at 5.6 meters for the destroyed, damaged, or possibly destroyed buildings. Meanwhile, DSM-derived height data commonly exceed these heights even in the cases of buildings identified as being destroyed by Copernicus EMS. Given that there are cases where OSM heights exceed DSM heights, it may be advantageous to adopt the greatest representative height from either the pre-event OSM height or the post-event DSM in future analyses.

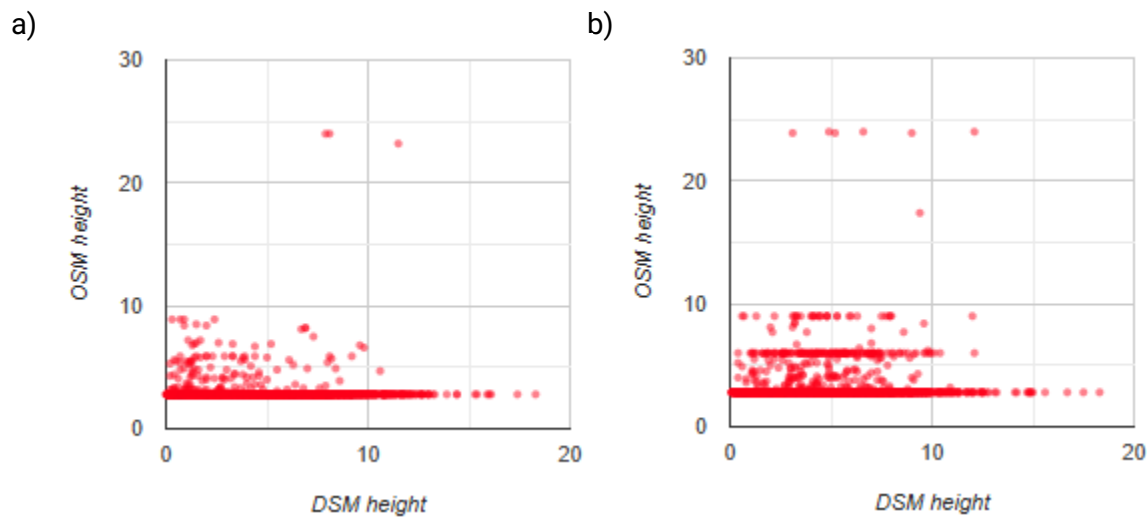


Figure 12. Comparison between OSM and DSM building height elevations for undamaged (a) and destroyed, damaged, or possibly damaged buildings (b) based on Copernicus EMS data.

We looked into the possibility of categorizing damage purely based on the DSM height differences but struggled to find meaningful differences between the height trends and overall distributions within each Copernicus EMS-defined damage class. Considering Table 3 below, the maximum height across *destroyed* buildings is 15.7 meters with a median of 4.6 meters. Yet the maximum height across *undamaged* buildings is 17.8 meters with a median of 4.9 meters. We would expect a much starker difference in height metrics between destroyed and undamaged buildings but this is not the case. Across damage classes, there is an absence of differentiation in DSM heights that would be necessary to classify a building as being destroyed, damaged, or possibly damaged using the post-event DSM alone.

Categorizing damage based on DSM values alone might be possible by training an algorithm to identify meaningful differences in the distribution of height values within the building footprint potentially in comparison to height values immediately surrounding. For example, an undamaged building should express a narrow distribution of height values compared to a

partially damaged structure. Complicating this approach, a destroyed building would also have a narrow distribution of height values, albeit a lower typical height compared to an undamaged structure. Developing a meaningful heuristic to classify damage based on height distributions alone would require careful thinking and training using ground truth examples. Automating such an approach would also require exceptional spatial precision of building footprint and DSM datasets to isolate heights ‘inside’ and ‘surrounding’ a given building, which are likely not possible with the datasets used in this analysis.

Table 3. Comparison of summary statistics of building height (meters) across SAM building footprints grouped by Copernicus EMS damage class.

	Minimum	Maximum	Mean	Median	Standard deviation
Destroyed	0.3	15.7	4.8	4.6	2.3
Damaged	0.4	14.4	6.2	6.2	2.4
Possibly damaged	0.4	23.0	6.1	5.9	2.4
Not damaged	0.1	17.8	5.1	4.9	2.7

Estimation of debris volume and tonnage

We estimated building-level debris volume by focusing on SAM building footprints identified as damaged by the Sentinel-1 CCD analysis above. A common method for estimating gross debris volume across a study area uses the following equation:

$$R = D * V * F * M$$

Where:

- R is the total volume of rubble or debris (m^3)
- D is the average damage percentage factor, ranging between 0 (no damage) - 1 (totally destroyed)
- V is the total pre-event volume of structures (m^3)
- M is the material mass (factor of mass * material stock) of the built structures (percentage of the total volume which is occupied by material which can turn into debris), ranging between 0 (no material mass) - 1 (100% material mass in volume).

Since we lack information on pre-Beryl building volumes, we developed an alternative estimation approach using the following equation:

$$R = V_{loss} * M$$

Where:

- R is the total volume of rubble or debris (m^3)
- V_loss is the loss in volume of built structures (m^3)
- M is the material mass (factor of mass * material stock) of the built structures (percentage of the total volume which is occupied by material which can turn into debris), ranging between 0 (no material mass) - 1 (100% material mass in volume).

We measured V_loss based on the difference between the footprint's maximum elevation and the elevation at each 1 meter resolution DSM pixel within a given SAM building footprint. This measure provided a pixel-level estimate of the height difference between the building surface and its nominal roof height (the maximum value per footprint). Multiplying this height by the pixel resolution provided a virtual volumetric column of debris per pixel. We then added all volumetric columns within each building footprint to estimate building footprint level volume.

We adopted a fixed factor of mass for each building of 0.1. This means that only 10% of each building is assumed to be taken up with building materials that could become rubble or debris, while the rest is empty space. This rule of thumb estimate is an oversimplification since the factor of mass will vary greatly by building type and design, but is nonetheless commonly employed lacking any other information.

To convert this to material-specific debris volume and then tonnage, we needed additional information on the material stock contributions of common materials used in construction across the study area. We referenced material intensity values from the Material Intensity Database (https://github.com/nheeren/material_intensity_db), isolating values for Grenada. We identified concrete, aggregate, steel, and wood as being common construction materials in Grenada, calculated their respective average contributions to the volume of building materials, as well as their representative densities (Table 4). Multiplying the respective contributions of each material to the total debris volume yields estimates of debris volume for each material (Table 5). Finally, multiplying the density of each material to its volume yields an estimate of debris tonnage per material and in total.

Applying this approach, we estimated a total volume of debris material of 50953 m^3 and total debris mass of 134943 tons across all SAM building footprints identified as being damaged or destroyed by the Sentinel-1 CCD analysis.

Table 4. Summary of material type characteristics derived from Grenada data in the Material Intensity Database (https://github.com/nheeren/material_intensity_db).

Material type	Contribution to volume of building material (%)	Representative density (kg/m^3)
Concrete	78.7	2400
Aggregate	9.5	2400
Steel	6.4	7800

Wood	5.4	600
------	-----	-----

Table 5. Estimates of material-specific debris volume and tonnage.

Material type	Debris volume (m ³)	Debris mass (tons)
Concrete	40100	96240
Aggregate	4841	11617
Steel	3261	25436
Wood	2751	1651
Total	50953	134943

Summary and Recommendations

Estimating debris volume and mass following Hurricane Beryl highlights both the utility and limitations of current remotely sensed data and standard modeling approaches. We found that OpenStreetMap (OSM) building height data were unreliable for volumetric analysis, with more than 90% of structures assigned a default minimum height of 2.8 meters—an evident data artifact that severely underrepresents building dimensions. While the post-event Pleiades DSM provided a richer distribution of building heights, it cannot be used alone to infer damage status, as many damaged or even destroyed structures retain elevation values comparable to undamaged ones. Furthermore, relying solely on the DSM to calculate volume loss risks misclassification, especially in small or irregular structures typical of the Caribbean built environment.

Our findings suggest value in combining both height sources, taking the maximum of OSM- or DSM-derived heights for each structure as a more robust estimate of pre-disaster building height. However, this does not resolve a key limitation: the absence of detailed information on building type, structural composition, and materiality across the study area. These gaps introduce uncertainty into the estimation of material-specific debris volumes and overall tonnage. Our use of a standard mass factor (10%) and generic material intensity values, while methodologically common, likely underestimates the true volume and weight of debris—particularly in cases where damage was missed due to the limits of radar-based detection.

Recommendations:

1. Further develop hybrid methodologies like those shown in this report that incorporate all-available open and commercial geospatial products to fully support recovery operations and material logistics planning.

2. Integrating multi-source height data using the maximum observed pre- or post-event height as a proxy for original building height.
3. Supplementing remote assessments with on-the-ground or ancillary data on building types and materials, especially in regions with high construction variability.
4. Developing more nuanced algorithms to interpret DSM height distributions within and around building footprints for more accurate damage classification.
5. Prioritizing the acquisition of VHR SAR or lidar data where feasible, to enhance vertical accuracy and reduce reliance on assumptions.
6. Treating current volume and tonnage estimates as conservative baselines, with the understanding that undetected damage and limited material data likely bias outputs downward.

Data shared in repo

- *DSM_heights_[class].csv*: DSM-derived building heights for SAM building footprints, sorted by Copernicus EMS damage class. Used to make Figure 11.
- *onegeo.shp*: OSM building footprints with building height attribute
- *OSM_vs_DSM_[class].csv*: OSM building footprint-level comparison of OSM height and DSM height. Used to make Figure 12.
- *sam_V_material_sar.shp*: SAM building footprints identified as damaged by SAR with attribute information on building material volume and tonnage.